

Effect of Arc Strikes on High Strength Low Alloy Steels Welded by SMAW

Dariusz Fydrych¹, Przemysław Raczko², Aleksandra Świerczyńska^{1*},
Michał Landowski¹, Adrian Wolski¹, Grzegorz Rogalski¹

¹ Institute of Manufacturing and Materials Technology, Faculty of Mechanical Engineering and Ship Technology, Gdańsk University of Technology, Gabriela Narutowicza Street 11/12, 80-233 Gdańsk, Poland

² S.N.SINEMA, Opata Hackiego Street 8-10, 81-213 Gdynia, Poland

* Corresponding author's e-mail: aleksandra.swierczynska@pg.edu.pl

ABSTRACT

Wet welding with covered electrodes (Shielded Metal Arc Welding – SMAW) is the most commonly used method of carrying out welding repair works in a water environment. Limited visibility and the inability to move freely under water result in an increased risk of formation of welding imperfections such as lack of fusion, lack of penetration and arc strikes. The work focused on changes in the properties and structure of steel subjected to the impact of short (0.2 s) arc ignitions generated by covered electrodes in air and under water for three high strength steel grades: S460N, S460M and S500MC. Visual tests, macroscopic and microscopic metallographic tests, microhardness measurements and diffusible hydrogen content in deposited metal determination were performed. A significant influence of the environment on changes in the morphology and microhardness of steel in the vicinity of arc strikes was found. The microhardness of the areas covered by the rapid thermal cycle caused by SMAW increased from 200–230 HV0.5 to 400–500 HV0.5 depending on the steel grade. The presence of welding imperfections: cavities and cracks were detected. The susceptibility of all steel grades subjected to short thermal cycles to cracking was confirmed by the results of measurements of the diffusible hydrogen content: 38.6 ml/100 g and 84.5 ml/100 g for air and water environment, respectively. No influence of changes in the welding current on the behavior of the material in the tested conditions was found. The conducted research shows that leaving arc strikes on the structure may have serious consequences and cause a failure.

Keywords: arc strikes, underwater welding, SMAW, covered electrode, high strength steel, diffusible hydrogen

INTRODUCTION

Welding processes are included in the group of special processes that require formalized supervision, which results, among others, from the ISO 9001 standard, and is included in detail in EN ISO 3834 [1, 2]. For this reason, much attention is paid to the issues of ensuring the quality of welded joints. In particular, the topics related to the maintenance of the documentation, training of welders, qualification of welding technologies, creation of welding procedure specifications, supervision of welding equipment, storage and distribution of welding consumables are discussed [3, 4]. It is important to monitor the welding

process not only in terms of arc voltage and welding current parameters, but also considering the quality of the work performed. These issues are particularly important during welding of metals of limited weldability, especially in extreme conditions: arctic, field (e.g. during the fabrication of transmission pipelines) and under water [5-9]. Welding under water can be carried out using the dry method, local dry cavity or with direct contact of the welding area with water [10-12]. Water, due to its diametrically different physical and chemical properties from air, is an environment that generates specific problems affecting the weldability of steel. The most important phenomena in this regard include: increased diffusible

hydrogen content, limited visibility, reduced arc stability and increased cooling rate resulting from significant differences in coefficients determining heat distribution, e.g. heat transfer [13-15]. The impact of short welding thermal cycles on steels with increased hardenability under hydrogenation conditions is the basic cause of the formation of cold cracks [16, 17].

The PN-EN ISO 6520-1:2009 standard classifies geometric welding imperfections in metals, dividing them into 6 groups: 1 – cracks, 2 – cavities, 3 – solid inclusions, 4 – lack of fusion and penetration, 5 – imperfect shape and dimensions, 6 – miscellaneous imperfections [18]. All welding imperfections not included in groups 1 to 5 are miscellaneous. They relate to the surface condition, external shape or geometry of the joint and are detected by visual tests and simple measurements [19-23]. In this group the standard includes, among others, grinding marks, spatter and arc strike.

The arc strike is defined as a local damage to the surface of the base material, most often in the vicinity of the weld, caused by arc ignition outside the weld groove [24, 25]. The imperfection may be due to the electrode, electrode holder or ground clamp coming into contact with the material. The main reason for the occurrence of arc strikes is the lack of qualifications of the welder or lack of diligence in the manufacturing of the joint [26]. In accordance with the guidelines of the EN ISO 5817 standard and most technical specifications of the customer, this imperfection is unacceptable at B and C levels, while at D level it is acceptable provided that it does not affect the properties of the base metal. It follows that in the case of steel with increased hardenability, even at the D quality level, this type of imperfection is not acceptable.

Arc strikes are mainly formed during welding with covered electrodes. It is a process commonly used in field conditions, to perform repair works on castings of ferrous and non-ferrous alloys and for welding of steel constructions operated under water [13, 19, 27-29]. Working in a water environment, which is denser than air, significantly reduces movement and visibility. This is conducive to the formation of welding imperfections from groups 5 and 6, including arc strikes.

The state of the art regarding arc strikes includes the regulations of classification societies and a few scientific articles. According to the DN-VGL-OS-C401 guidelines [30]: “arc strikes shall

be repaired by mechanical removal of affected base material followed by Magnetic Particle Testing (MT) in order to verify absence of cracks”. Removal of arc strikes usually requires a grinding process. This generates a reduction in the thickness of the element at the grinding site, which is associated with a change in the dimension of the cross-section. In a situation where this reduction is below the required minimum, a given element, and in justified cases a fragment of an element, should be replaced. The acceptance limits for unrepaired arc burns (including arc strikes) are given in API 1104 standard. An additional, general requirement is that arc burns that contain cracks visible to the eye or on conventional radiographs should be repaired or removed.

The assessment of the influence of arc strikes on the mechanical, technological and operational properties of metals is extremely rare in the literature. The authors of [25] described studies of simulated imperfections performed on high strength steel, concluding that they could be dangerous for the durability of the structure. In particular, strikes are potential fatigue initiation sites [26]. The paper [31] describes the results of the failure analysis of a high carbon steel post-tensioned threadbar. After determining that the most probable cause of the failure of the element was the presence of arc strike, metallographic and strength tests of the material with artificially made imperfections were carried out. It was found, that the effect of the thermal cycle caused a significant increase in the hardness of the material as well as the formation of brittle structures and cavities in molten area of material, which suggests hydrogenation of the specimens and an increase in the tendency of steel to cold cracking.

The aim of the research was to determine and compare changes in the structure and properties of high strength steels caused by arc strikes in air and water environment.

MATERIALS AND METHODS

The scope of work included the controlled fabrication of imperfections (arc strikes) on the surface of three high strength low alloy steel grades in air and under water, and the implementation of visual observations, macro- and microscopic metallographic tests, microhardness measurements and diffusible hydrogen content in deposited metal determination.

Three grades of unalloyed steels used in the marine and off-shore industry were selected for the tests: S460N, S460M and S500MC with a thickness of 15 mm each. The chemical composition and carbon equivalent values of the tested steel grades are summarized in Table 1. The yield strength, tensile strength and elongation of the tested steel grades are summarized in Table 2. Selected steel grades differ slightly in yield strength (511–525 MPa), while the value of carbon equivalent is strongly differentiated (from 0.31 to 0.49 %), which proves good weldability of thermomechanically rolled steels and limited weldability of normalized steel. Specimens with dimensions of 100x100 mm were prepared, on which arc strikes were made manually (according to production practice) using rutile coated electrodes ER 1.50 Ø 3.25 (PN-EN ISO 2560-A:E 38 0 RC 11, AWS A5.1: E 6013) with DCEN polarity. An ESAB Aristo 4001i welding machine was used.

Each specimen was marked with five arc strikes made with the value of the current increasing by 20 A from 90 to 170 A. A maximally wide range of welding current was selected based on the data recommended by the manufacturer of the electrodes and a step of 20 A reflected the practical possibility of setting welding parameters. The actual, average current values read from the device were respectively: 92 A, 112 A, 132 A, 152 A, 172 A. To test all of the materials the arc strike time (welding current flow) recorded with the Kemppi DataCatch measurement module was constant and it was 0.2 s.

First, specimens were made in air environment, and then – on the other side of the specimen – by underwater wet welding. This allowed

to obtain double-sided specimens, which were marked with the letter A for air or W for water and the symbol of the steel grade. Figure 1 shows the scheme of the underwater welding test stand, while Figure 2 shows the scheme of the specimen.

The surface of the specimens was visually tested in accordance with ISO 17637 standard, then specimens were cut out for macro- and microscopic metallographic examinations. Metallographic cross sections were prepared using a standard procedure: they were ground on waterproof sandpaper with a gradation of 200 to 2000, and then chemically etched with Nital (4% solution of nitric acid in ethyl alcohol). An Olympus BX51 optical system microscope was used for microscopic observations and measurements of the dimensions of the imperfections. The microhardness distribution across the specimen according to scheme presented in Figure 3 was determined

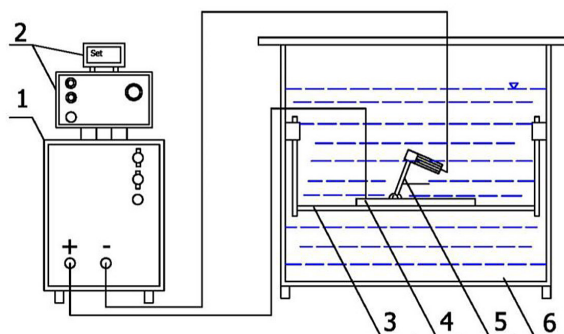


Figure 1. Scheme of the underwater welding test stand: 1 – welding machine, 2 – control panel, 3 – welding table, 4 – specimen, 5 – electrode, 6 – water container [32]

Table 1. Chemical composition and carbon equivalent value of tested steels and deposited metal of electrode

| Designation | C | Mn | Si | P | Cr | Mo | Ni | Al | Cu | Nb | Ti | V | CE _{IW} |
|-------------|------|-----|------|------|------|------|------|------|------|------|------|------|------------------|
| S460N | 0.16 | 1.6 | 0.5 | 0.07 | 0.02 | 0.03 | 0.06 | 0.03 | 0.14 | - | 0.01 | 0.11 | 0.49 |
| S460M | 0.11 | 1.6 | 0.5 | - | 0.02 | 0.01 | 0.03 | - | - | 0.03 | - | 0.01 | 0.38 |
| S500MC | 0.07 | 1.4 | 0.02 | - | - | - | - | 0.04 | - | 0.06 | - | 0.05 | 0.31 |
| ER 1.50 | 0.09 | 0.5 | 0.3 | - | - | - | - | - | - | - | - | - | - |

Note: $CE_{IW} = C + Mn/6 + (Cr + Mo + V)/5 + (Ni + Cu)/15$

Table 2. Mechanical properties of tested steels and deposited metal of electrode

| Designation | Re [MPa] | Rm [MPa] | A ₅ [%] |
|-------------|----------|----------|--------------------|
| S460N | 511 | 626 | 27.3 |
| S460M | 515 | 540-720 | 17 |
| S500MC | 525 | 619 | 20.5 |
| ER 1.50 | 380 | 470-600 | 20 |



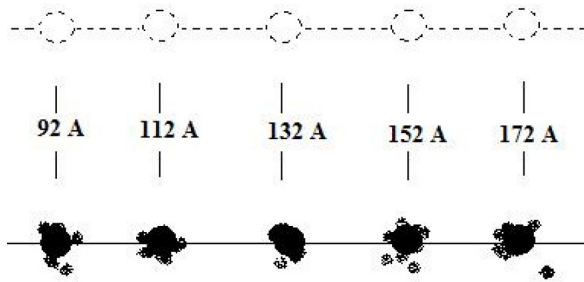


Figure 2. Scheme of the specimen with arc strikes

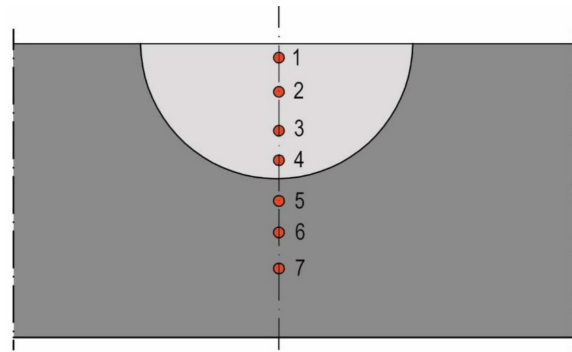


Figure 3. Scheme of microhardness measurements

on selected specimens by Vickers method, using Future-Tech FM-700 microhardness tester with a load of 0.5 kg and 15 s dwell time.

Diffusible hydrogen content in deposited metal in water and air environment was determined in accordance with EN ISO 3690 by high-temperature extraction using the Bruker G4 Phoenix analyzer. A piece assembly test made of non-alloy steel S355G10 with the dimensions of the central element: 10x15x30 mm was used to perform the measurements. Hydrogen extraction was carried out at 400°C for 30 min, and the average of 5 measurements was given as the result.

RESULTS AND DISCUSSION

Figure 4 shows photos of all specimens with arc strikes. In the case of imperfections made in

air environment, numerous spatters and a more regular oxidation zone with a larger width were found than in the case of arc strikes obtained in the water environment. There was no relationship between the value of welding current and the diameter of arc strikes.

An example of a macroscopic cross-sections of arc strikes made on each specimen is shown in Figure 5. It was noted that the traces of arc strikes, despite the short time of arc burning, consist of a shallow zone of weld metal and a heat affected zone. The surface of the imperfections is very irregular, which may indicate the presence of internal defects.

The results of measurements of dimensions of arc strikes are shown in Table 3. The comparison of imperfections made in different environments shows that in most cases the arc strikes that were made under water have larger dimensions (width

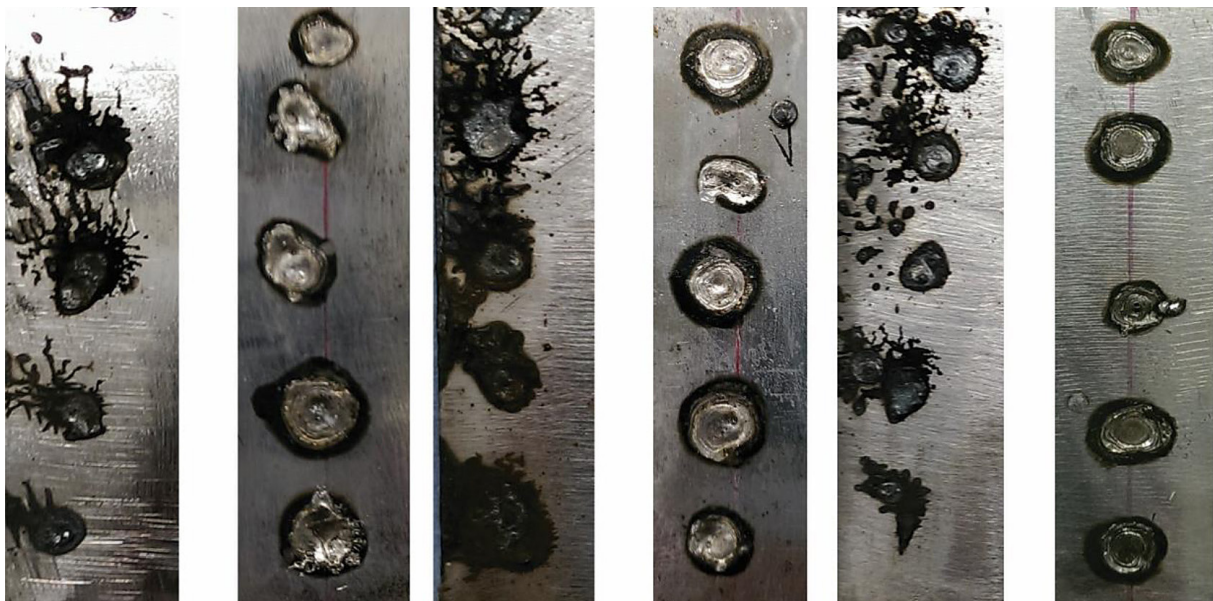


Figure 4. Top view of specimens with arc strikes: a) A460N, b) W460N, c) A460M, d) W460M, e) A500M, f) W500M

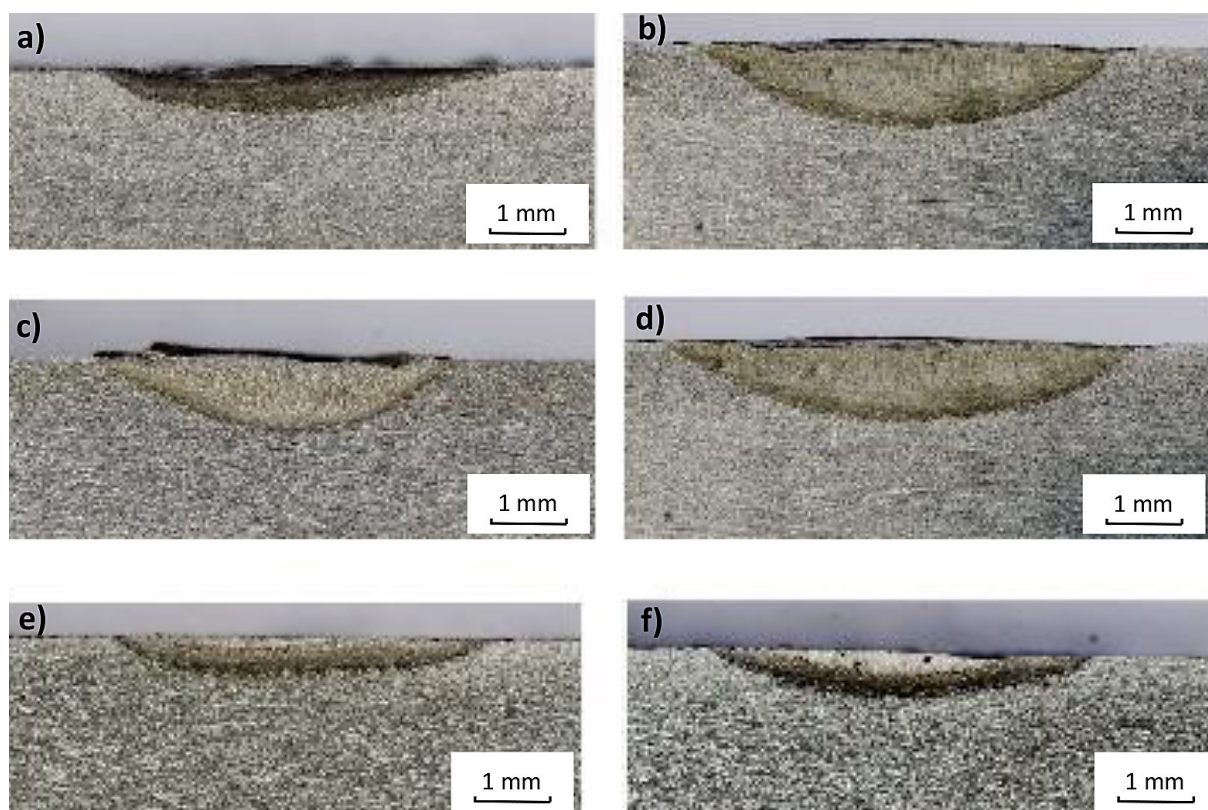


Fig. 5. Macroscopic cross-section of specimens with arc strikes: a) A460N, b) W460N, c) A460M, d) W460M, e) A500M, f) W500M

and depth) than their counterpart from the air. The API 1104 standard states that the total depth of the arc strike, including the heat-affected zone, is less than half the width of the strike. The results presented in Table 3 confirm this relationship.

Numerous imperfections were found during microscopic examination: mainly cavities (Figures 6c and e) and cracks (Figure 6d). In some cases, cracks and cavities occurred simultaneously (Figures 6a and b). The high concentration of imperfections, both for specimens made in air and under water, indicates a rapid course of phenomena occurring during the formation of arc strikes, resulting in the formation of brittle structures and high stress value.

The analysis of microhardness distributions (Figure 7) shows that the rapid thermal cycle caused a significant increase in the microhardness of all steel grades, to the level of: 400–420 HV0.5 for S460M and S500M steels and over 500 HV0.5 for S460N steel grade. The highest microhardness was noted at the surface of the specimens and it decreased in the direction of the measurements to the value characteristic of the base material (about 200–230 HV0.5).

In all cases, the microhardness of the specimens made under water was lower, which is an unexpected result, but it can be explained as follows: the process lasts too short to stabilize

Table 3. The results of measurements of dimensions of arc strikes

| Specimen | 92 A | | 112 A | | 132 A | | 152 A | | 172 A | |
|----------|------------|------------|------------|------------|------------|------------|------------|------------|------------|------------|
| | width [mm] | depth [mm] | width [mm] | depth [mm] | width [mm] | depth [mm] | width [mm] | depth [mm] | width [mm] | depth [mm] |
| A460N | 5.12 | 0.33 | 4.23 | 0.44 | 5.43 | 0.55 | 5.43 | 0.55 | - | - |
| W460N | - | - | 5.25 | 0.83 | 5.73 | 1.07 | 5.87 | 0.95 | 6.7 | 1.22 |
| A460M | 5.15 | 0.92 | 3.99 | 0.79 | 4.37 | 0.93 | 5.38 | 0.84 | 4.98 | 0.78 |
| W460M | 6.23 | 1.15 | 4.46 | 0.92 | 5.70 | 1.09 | 5.7 | 0.95 | 3.63 | 0.65 |
| A500MC | 1.42 | 0.25 | 3.54 | 0.45 | 5.11 | 0.81 | 4.31 | 0.58 | 2.71 | 0.45 |
| W500MC | 3.23 | 0.64 | 4.44 | 0.81 | 5.56 | 1.01 | 5.07 | 0.86 | 4.11 | 0.65 |

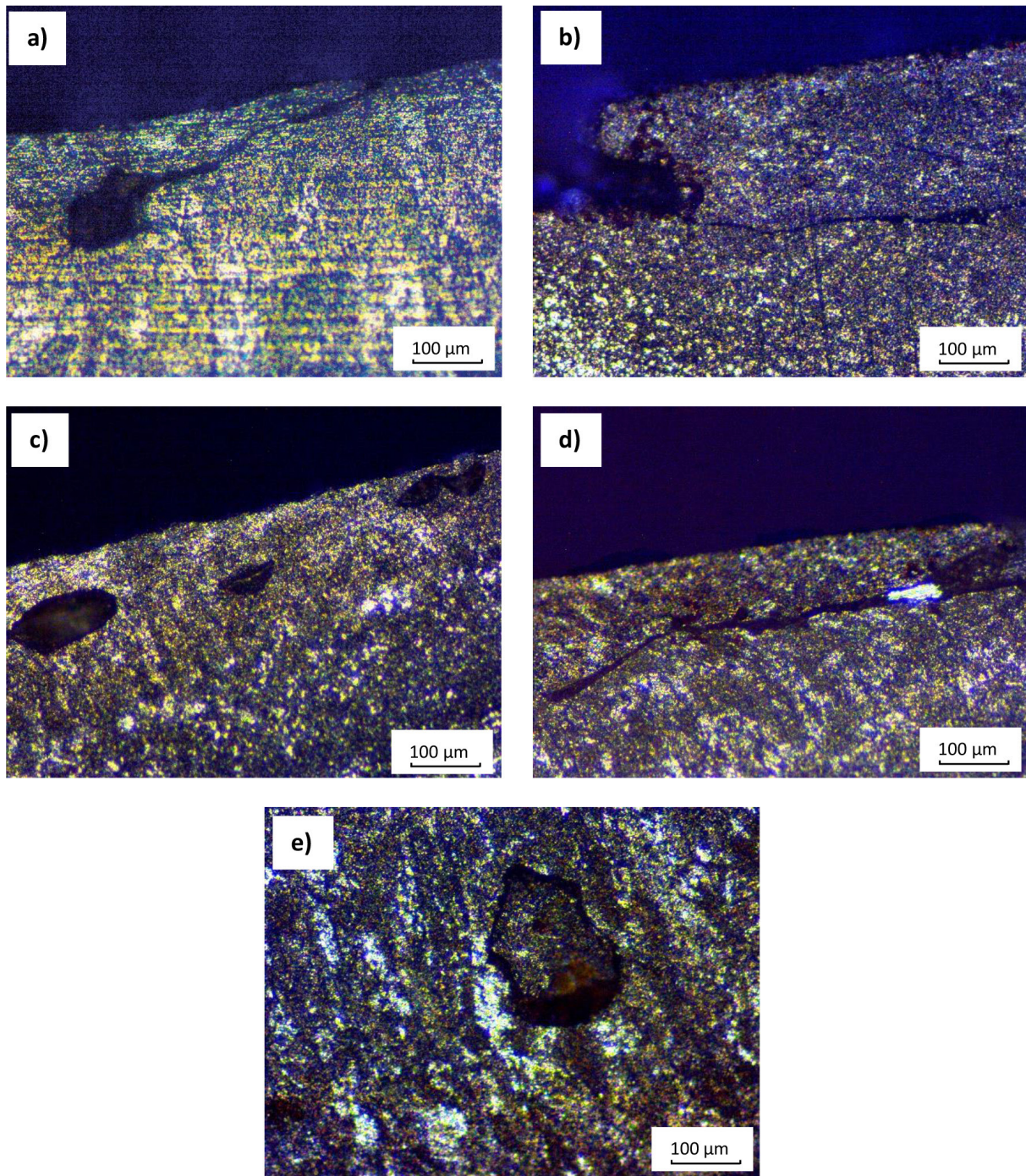


Figure 6. Microscopic view of defects in arc strikes: a) cavity and crack (W460M), b) crack (W460N), c) cavities (A500M), d) crack (W500M), e) cavity (W500M)

the arc and the cooling effect of water is negligible compared to the temperature gradient caused by plates of considerable thickness. A strong relationship was found between the carbon equivalent value and the maximum microhardness in both water ($R^2=0.86$) and air ($R^2=0.90$) environments (Figure 8).

Figure 9 shows a view of specimens for determination of diffusible hydrogen content in deposited metal in air and water environments.

The average hydrogen levels were 38.6 ml/100g and 84.5 ml/100g for air and water, respectively, and these are consistent with literature data for welding with rutile covered electrodes [33, 34].

The determined high diffusible hydrogen amount significantly exceeds the highest level of the hydrogen scale (H15) and suggests that the tested steel grades subjected to rapid cooling may have a high tendency to cracking.

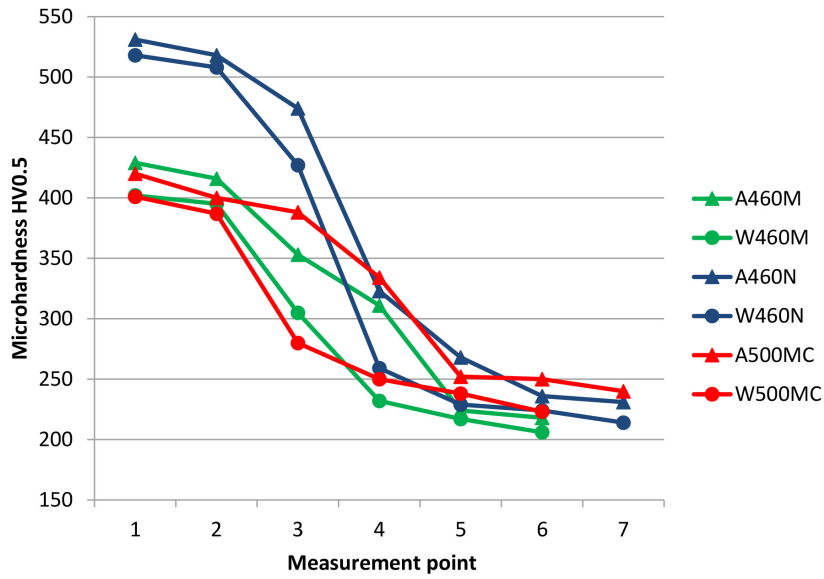


Figure 7. Microhardness distributions in the area of arc strikes

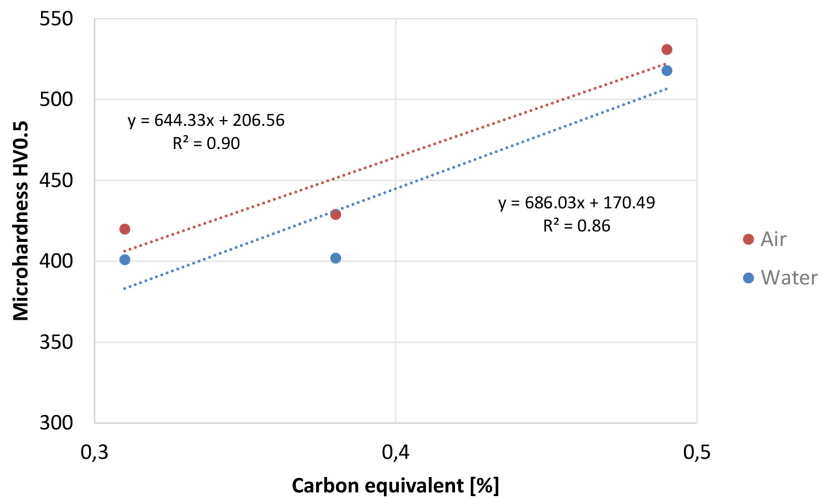


Figure 8. Dependence of microhardness on the value of carbon equivalent



Figure 9. Specimens for determination of diffusible hydrogen content in deposited metal

CONCLUSIONS

According to the results of the analysis carried out and industrial experience, it can be concluded that the environment and steel grade significantly affect morphology and properties of metal subjected to rapid thermal cycle [34]. Arc strikes are a highly disregarded welding imperfection among the unacceptable ones. The issue is surprisingly rarely addressed in both literature and production practice.

Limited visibility during underwater welding work favors the formation of strikes, and the rapid cooling rate increases the microhardness within the imperfections. A short impact of a small amount of heat on a metal with a relatively large capacity causes the formation of a wide temperature gradient, which, acting locally, causes structural transformations resulting in a change in properties. Brittle, susceptible to cracking structures are formed. An accurate calculation of the cooling rate of arc strike, especially in underwater conditions, is currently probably impossible. Appropriate formulas and conditions for numerical methods (FEM) are not known. Wang et al. [35] stated that for underwater wet welding of steel, the cooling time in the temperature range of 800–500 ($t_{8/5}$) is about 5 s. It can be assumed that the cooling rate described by $t_{8/5}$ during arc strike is much lower than 1 s, which must lead to microhardness exceeding 350 HV. This is consistent with the results obtained in current studies (Figures 7 and 8). In the case of the tested steel grades, it can be concluded that the cooling time for the tested steel grades is practically identical and probably does not depend significantly on the process environment. The high level of hydrogenation (38.6 ml/100g and 84.5 ml/100g) of the quenched structures formed by arc strikes suggests that the discovered cracks were formed by a mechanism characteristic of the cold cracking phenomenon.

No influence of welding current changes on the behavior of the material was found, which is probably due to the fact that the arc strike is formed at the arc start stage, when the value of the welding current are not yet stabilized. The arc strike area cannot be considered as a weld. The short duration of the process does not allow the arc to stabilize and limits the amount of metal transported in the arc.

Although the influence of the steel grade on the intensity of imperfections in metal areas

subjected to rapid thermal cycle impact has not been confirmed, the relationship between the maximum microhardness and the value of carbon equivalent has been demonstrated.

Based on the results of visual examinations, it can be concluded that making arc strikes in air environment resulted in numerous spatters and the formation of an oxidation zone with a larger area than during the experiments in the water environment. The influence of the environment was not visible during the analysis of internal imperfections: cavities and cracks appeared both in the specimens made in air and under water, regardless of the value of the welding current and the steel grade. An interesting observation was that the microhardness of the material subjected to the rapid thermal cycle under water is lower than for specimens made in air environment.

It should be stated that the considered steel grades welded under water and in air are susceptible to formation of arc strikes. It should be emphasized that the detection of these defects and the use of the proposed methods of removing these imperfections under water are significantly limited or even impossible. Therefore, during the training of welders, they should be made aware of the serious consequences for the service life of the structure that carelessness during welding and ignoring the observed imperfections can have.

The analysis of the presented results shows that it is necessary to comply with the guidelines for grinding and conducting non-destructive surface tests in the case of welding the tested steel grades. Leaving arc strike on the element may pose a serious threat to the service life of the structure [23, 36, 37].

Acknowledgments

Authors would like to thank Dr. Jacek Bielawski for inspiration and valuable discussions.

REFERENCES

1. Mitelea I., Bordeasu I., Cosma D., Uțu I.D., Crăciunescu C.M. Microstructure and Cavitation Damage Characteristics of GX40CrNiSi25-20 Cast Stainless Steel by TIG Surface Remelting. *Materials* 2023, 16(4): 1423.
2. Brätz O., Henkel K.M. Investigations on the microstructure of drawn arc stud welds on structural steels by quantitative metallography. *Welding in the World*

- 2023, 67(1): 195-208.
3. Świerczyńska A. Effect of storage conditions of rutile flux cored welding wires on properties of welds. *Advances in Materials Science* 2019, 19(4): 46-56.
 4. Samadi F., Mourya J., Wheatley G., Khan M.N., Nejad R.M., Branco R., Macek, W. An investigation on residual stress and fatigue life assessment of T-shape welded joints. *Engineering Failure Analysis* 2022, 141: 106685.
 5. Szymczak T., Szczucka-Lasota B., Węgrzyn T., Łazarz B., Jurek A. Behavior of weld to S960MC high strength steel from joining process at micro-jet cooling with critical parameters under static and fatigue loading. *Materials* 2021, 14(11): 2707.
 6. Mičian M., Winczek J., Harmaniak R., Koňár R., Gucwa M., Moravec J. Physical simulation of individual heat-affected zones in S960MC steel. *Archives of Metallurgy and Materials* 2021, 66(1): 81-89.
 7. Węgrzyn T. The classification of metal weld deposits in terms of the amount of oxygen. *Proceedings of the Ninth International Offshore and Polar Engineering Conference, Brest, France, 1999.*
 8. Moreno-Urbe A.M., Bracarense A.Q., Pessoa E.C. The effect of polarity and hydrostatic pressure on operational characteristics of rutile electrode in underwater welding. *Materials* 2020, 13(21): 5001.
 9. Fajt D., Maślak M., Stankiewicz M., Zajdel P., Pańcikiewicz K. Influence of Long-Term Subcritical Annealing on the Unalloyed Steel Welded Joint Microstructure. *Materials* 2023, 16(1): 304.
 10. Liu S., Ji H., Zhao W., Hu C., Wang J., Li H., Wang J, Lei Y. Evaluation of Arc Signals, Microstructure and Mechanical Properties in Ultrasonic-Frequency Pulse Underwater Wet Welding Process with Q345 Steel. *Metals* 2022, 12(12): 2119.
 11. Zhang X., Guo N., Luo W., Xu C., Tan Y., Fu Y., Cheng Q., Chen H., He J. A novel liquid-shielded welding solution for diffusible hydrogen content restriction and metal transfer controlling in underwater FCAW condition. *International Journal of Hydrogen Energy* 2022, 47(11): 7362-7367.
 12. Tomków J., Świerczyńska A., Landowski M., Wolski A., Rogalski G. Bead-on-plate underwater wet welding on S700MC steel. *Advances in Science and Technology Research Journal* 2021, 15: 288-296.
 13. Tomków J., Landowski M., Fydrych D., Rogalski G. Underwater wet welding of S1300 ultra-high strength steel. *Marine Structures* 2022, 81, 103120.
 14. Guo N., Zhang X., Xu C., Chen H., Fu Y., Cheng Q. Effect of parameters change on the weld appearance in stainless steel underwater wet welding with flux-cored wire. *Metals* 2019, 9(9): 951.
 15. Yang J., Xu S., Jia C., Han Y., Maksymov S., Wu C. A novel 3D numerical model coupling droplet transfer and arc behaviors for underwater FCAW. *International Journal of Thermal Sciences* 2023, 184: 107906.
 16. Klett J., Hassel T. Influence of stick electrode coating's moisture content on the diffusible hydrogen in underwater wet shielded metal arc welding. *Advances in Materials Science* 2020, 20(4): 27-37.
 17. Węgrzyn T., Szymczak T., Szczucka-Lasota B., Łazarz B. MAG welding process with micro-jet cooling as the effective method for manufacturing joints for S700MC Steel. *Metals* 2021, 11(2): 276.
 18. Brzeskot P., Łatka L. Development of the automatic method of detection and grouping of external welding imperfections. *Journal of Physics: Conference Series* 2022, 2412(1): 012012).
 19. Tomków J., Landowski M., Rogalski G. Application possibilities of the S960 steel in underwater welded structures. *Facta Universitatis, Series: Mechanical Engineering* 2022, 20(2): 199-209.
 20. Djatmiko R.D., Kurniawan D.A., Pratiwi H. Visual inspection on shielded metal arc welding products of Asian welding contestants in Yogyakarta province. *Journal of Physics: Conference Series* 2020, 1446(1): 012006.
 21. Kohandehghan A., Prescott J., Gues, S., Lepine S. An engineering assessment methodology to evaluate arc burns. *International Pipeline Conference, American Society of Mechanical Engineers, online* 2020, 84447, V001T03A021.
 22. Singh S., Singh A.B., Kumar M., Meena M.L., Dangayach G.S. Dissimilar metal welds used in AUSC power plant, fabrication and structural integrity issues. *IOP Conference Series: Materials Science and Engineering* 2021, 1017(1): 012022.
 23. Bhanu V., Gupta A., Pandey C. Role of A-TIG process in joining of martensitic and austenitic steels for ultra-supercritical power plants-a state of the art review. *Nuclear Engineering and Technology* 2022, 54(8): 2755–2770.
 24. Kasen M.B. Significance of blunt flaws in pipeline girth welds. *Welding Journal* 1983, 62(5): 117-122.
 25. Natarajan T.J., McCauley R.B. Arc strikes on high-strength steels. *Welding Journal* 1975, 54(12): 879-884.
 26. Gagg C.R., Lewis P.R. In-service fatigue failure of engineered products and structures – Case study review. *Engineering Failure Analysis* 2009, 16(6): 1775-1793.
 27. Žuk M., Górká J., Dojka R., Czupryński A. Repair welding of cast iron coated electrodes. *IOP Conference Series: Materials Science and Engineering* 2017, 227(1): 012139.
 28. Łabanowski J., Prokop-Strzelczyńska K., Rogalski G., Fydrych D. The effect of wet underwater welding on cold cracking susceptibility of duplex

- stainless steel. *Advances in Materials Science* 2016, 16(2): 68-77.
29. Hu Y., Shi Y., Wang K., Huang J. Effect of Heat Input on the Microstructure and Mechanical Properties of Local Dry Underwater Welded Duplex Stainless Steel. *Materials* 2023, 16(6): 2289.
30. Rhode M., Nietzke J., Mente T., Richter T., Kanngiesser T. Characterization of hydrogen diffusion in offshore steel S420G2+M multi-layer submerged arc welded joint. *Journal of Materials Engineering and Performance* 2022, 31(9): 7018-7030.
31. Chao J., Pena C. Effect analysis of an arc-strike-induced defect on the failure of a post-tensioned threadbar. *Case Studies in Engineering Failure Analysis* 2016, 5-6(4): 1-9.
32. Tomków J., Łabanowski J., Fydrych D., Rogalski G. Cold cracking of S460N steel welded in water environment. *Polish Maritime Research* 2018, 25(3 (99)): 131-136.
33. Tomków J., Fydrych D., Rogalski G., Łabanowski J. Effect of the welding environment and storage time of electrodes on the diffusible hydrogen content in deposited metal. *Revista de Metalurgia* 2019, 55(1): 140.
34. Wolski A., Świerczyńska A., Lentka G., Fydrych D. Storage of high-strength steel flux-cored welding wires in urbanized areas. *International Journal of Precision Engineering and Manufacturing-Green Technology* 2023 (In Press).
35. Wang J., Liu Y., Feng J., Sun Q. Microstructure evolution of E40 steel weldments in ultrasonic-wave-assisted underwater FCAW. *Welding Journal* 2021, 100: 106-120.
36. Otegui J.L., Fazzini P.G., Márquez A. Common root causes of recent failures of flanges in pressure vessels subjected to dynamic loads. *Engineering Failure Analysis* 2009, 16(6): 1825-1836.
37. Choudhury S.D., Li L., Saini N., Khan W.N., Ravikiran, K., Lyu Z. 3D characterization of internal defects for fatigue performance of welded SA192 steel water walls. *International Journal of Pressure Vessels and Piping* 2023, 202: 104922.

